Quantum and Nonlinear Optical Imaging

Robert W. Boyd

The Institute of Optics, University of Rochester

- The promise of quantum imaging
  (including quantum lithography)

- Imaging upconversion
  (for astronomy and for THz imaging)

- Nonlinear optical microscopy

Nonclassical, Two-Photon Interferometry and Lithography with High-Gain Optical Parametric Amplifiers

Robert W. Boyd, Elna M. Nagasako, Sean J. Bentley
University of Rochester, USA
and
Girish S. Agarwal,
Physical Research Lab., India

To what extent do unseeded, high-gain optical parametric amplifiers preserve the desirable quantum statistical properties of spontaneous parametric downconversion?

Quantum Lithography and Microscopy

- Entangled photons can be used to form interference patterns with detail finer than the Rayleigh limit
- Process "in reverse" performs sub-Rayleigh microscopy

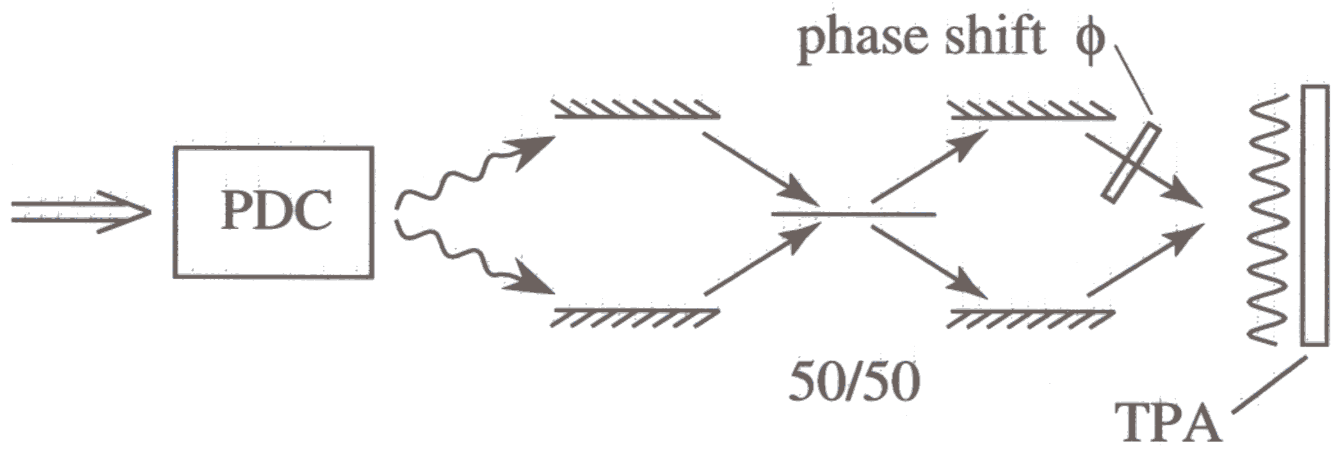

Boto et al, Phys. Rev. Lett. 85, 2733, 2000.

QUANTUM LITHOGRAPHY PROPOSAL

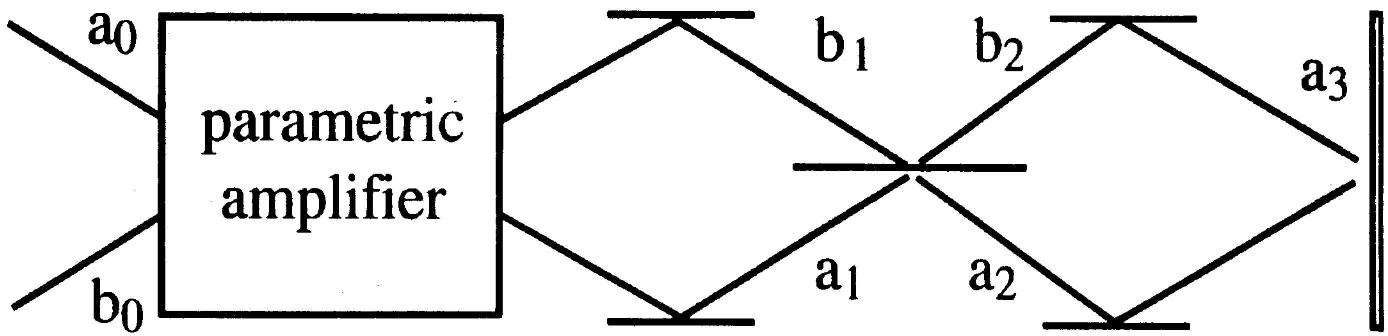

"Replace" parametric down converter (PDC) with optical parametric amplifier (OPA)–essentially the same device, but now pumped harder to generate sufficient energy levels to be recorded by two-photon responsive lithographic plate at a_3.

Use of High-Gain Parametric Amplifier

Is two-photon interference pattern preserved?

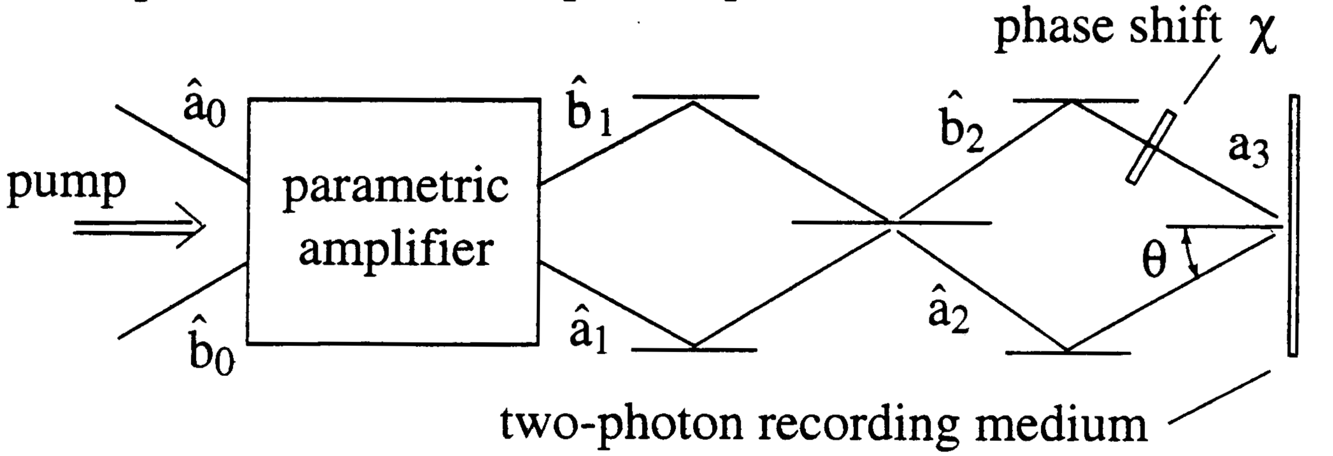

- Transfer equations of OPA

$$\hat{a}_1 = U\hat{a}_0 + V\hat{b}_0^\dagger, \quad \hat{b}_1 = U\hat{b}_0 + V\hat{a}_0^\dagger$$

where

$$U = \cosh G \qquad V = -\, i \exp(i\varphi) \sinh G$$

- Field at recording medium

$$\hat{a}_3 = \frac{1}{\sqrt{2}} \left[(-\,e^{i\chi} + i)(U\hat{a}_0 + V\hat{b}_0^\dagger) + (ie^{i\chi} - 1)(U\hat{b}_0 + V\hat{a}_0^\dagger)\right]$$

- Two-photon absorption probablility

$$\langle 0,0|\hat{a}_3^\dagger\hat{a}_3^\dagger\hat{a}_3\hat{a}_3|0,0\rangle = 4|V|^2\left[|U|^2\cos^2\chi + 2|V|^2\right]$$

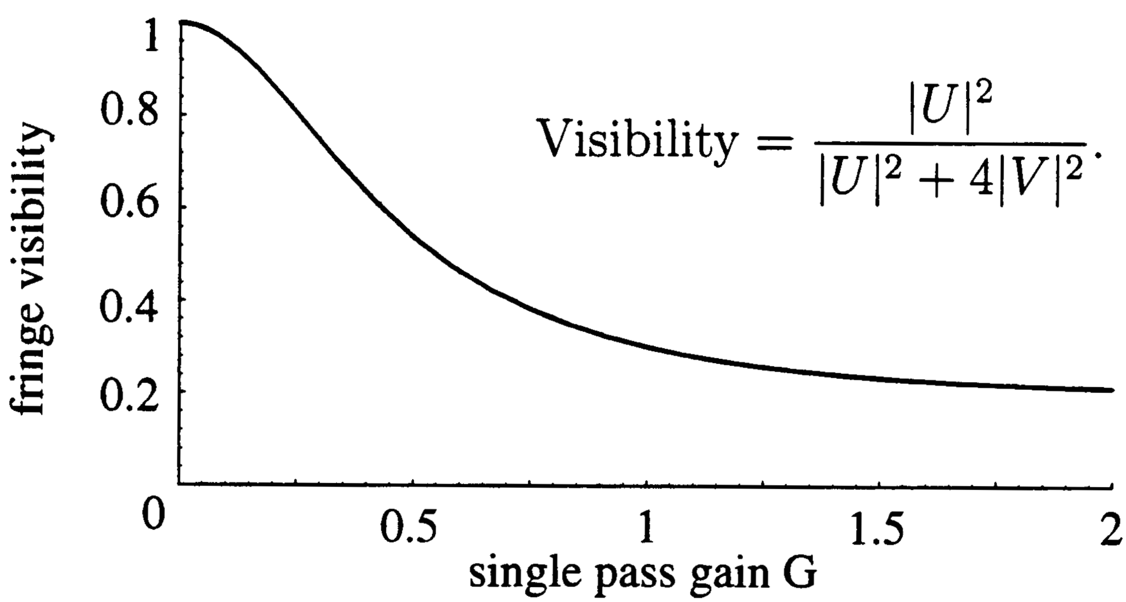

(Phys. Rev. Lett. 86, 1389, 2001)

QUANTUM LITHOGRAPHY PROPOSAL

Experimental Layout

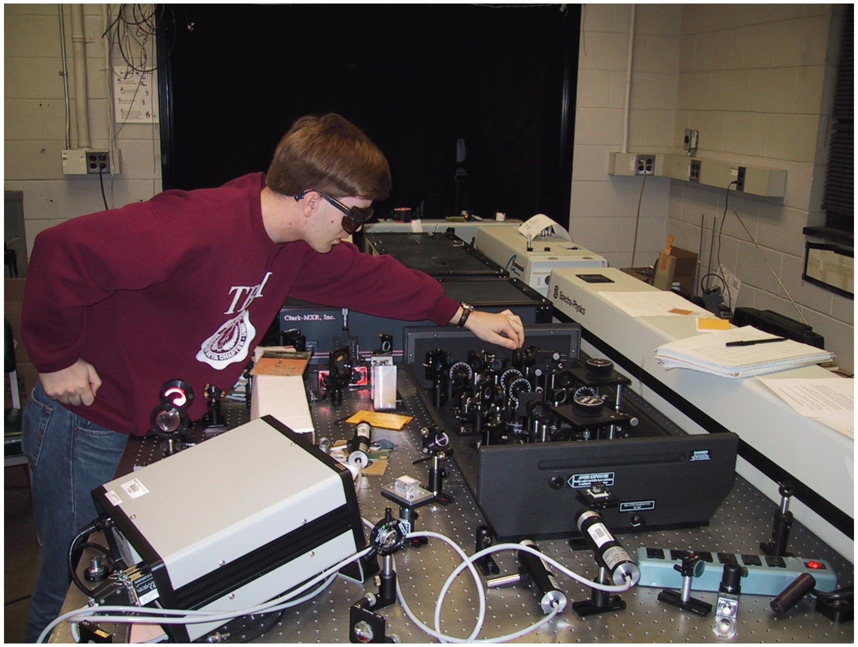

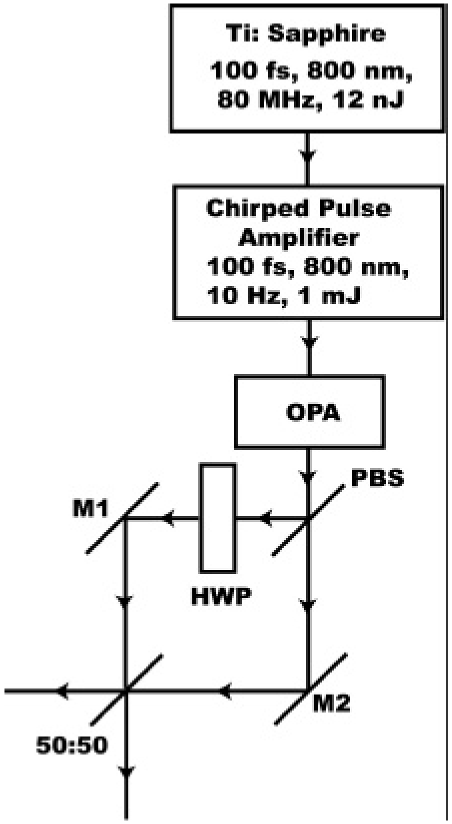

Hong-Ou-Mandel Interferometer

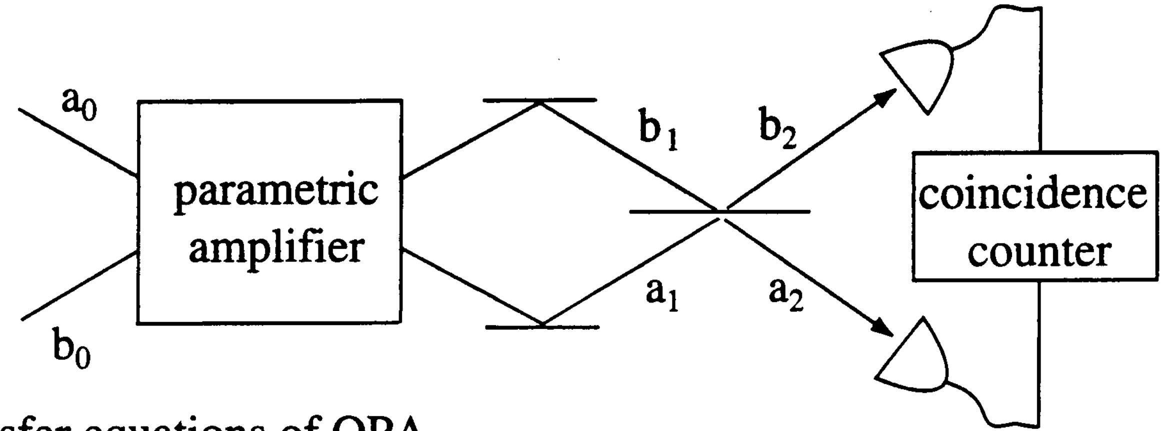

- Transfer equations of OPA

$$\hat{a}_1 = U\hat{a}_0 + V\hat{b}_0^\dagger, \quad \hat{b}_1 = U\hat{b}_0 + V\hat{a}_0^\dagger$$

where

$$U = \cosh G \qquad V = -\, i \exp(i\varphi) \sinh G$$

- Fields leaving the beamsplitter

$$\hat{a}_2 = \frac{1}{\sqrt{2}}[(U\hat{a}_0 + V\hat{b}_0^\dagger) - i(U\hat{b}_0 + V\hat{a}_0^\dagger)]$$

$$\hat{b}_2 = \frac{1}{\sqrt{2}}[-i(U\hat{a}_0 + V\hat{b}_0^\dagger) + (U\hat{b}_0 + V\hat{a}_0^\dagger)]$$

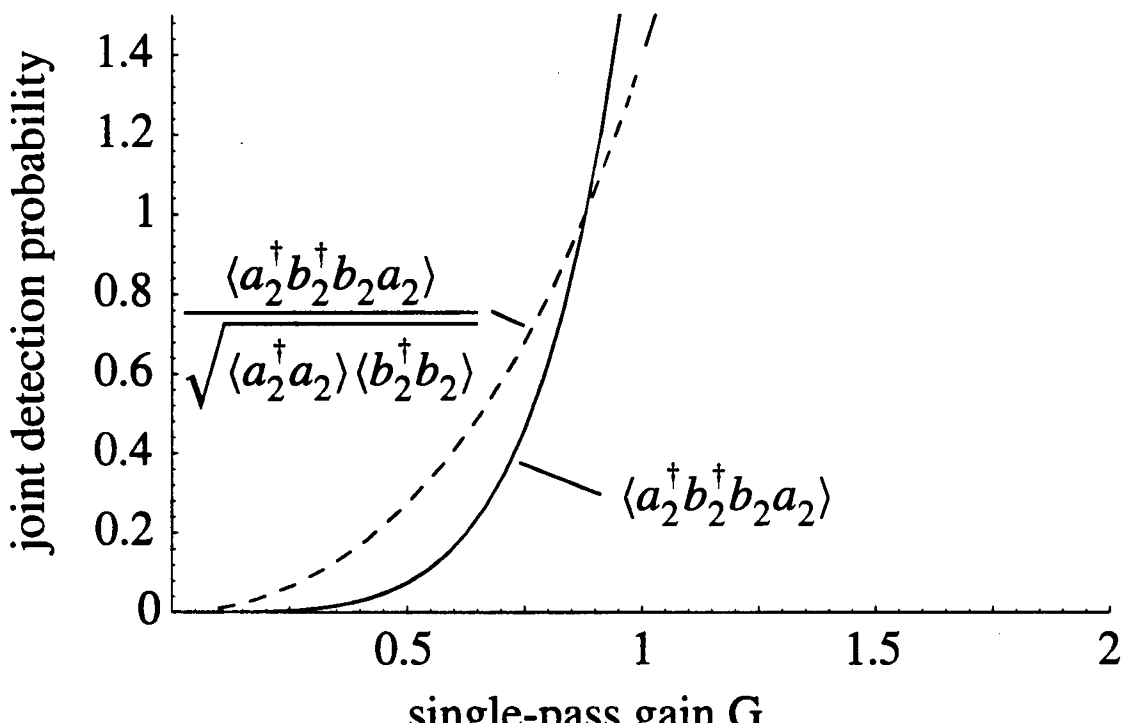

Mach-Zehnder Coincidence-Count Statistics

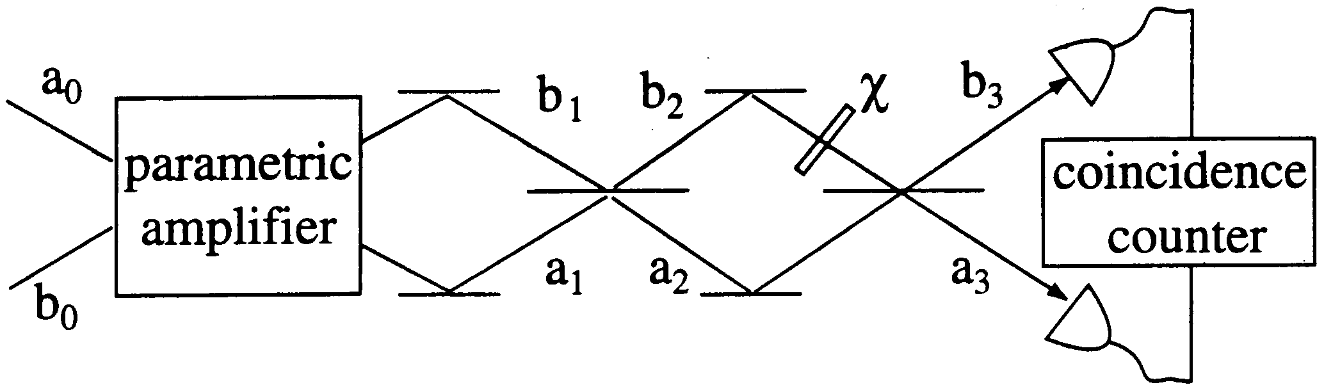

- Transfer equations of OPA

$$\hat{a}_1 = U\hat{a}_0 + V\hat{b}_0^\dagger, \quad \hat{b}_1 = U\hat{b}_0 + V\hat{a}_0^\dagger$$

where

$$U = \cosh G \qquad V = -\, i\exp(i\varphi)\sinh G$$

- Fields at detectors

$$\hat{a}_3 = \tfrac{1}{2}[(1-e^{i\chi})(U\hat{a}_0 + V\hat{b}_0^\dagger) - i(1+e^{i\chi})(U\hat{b}_0 + V\hat{a}_0^\dagger)]$$

$$\hat{b}_3 = \tfrac{1}{2}[-i(1+e^{i\chi})(U\hat{a}_0 + V\hat{b}_0^\dagger) - (1-e^{i\chi})(U\hat{b}_0 + V\hat{a}_0^\dagger)]$$

- Joint detection probability

$$\langle \hat{a}_3^\dagger \hat{b}_3^\dagger \hat{b}_3 \hat{a}_3 \rangle = |V|^2 \left[\tfrac{1}{2}(1+\cos 2\chi) + |V|^2(\tfrac{3}{2} + \tfrac{1}{2}\cos 2\chi)\right]$$

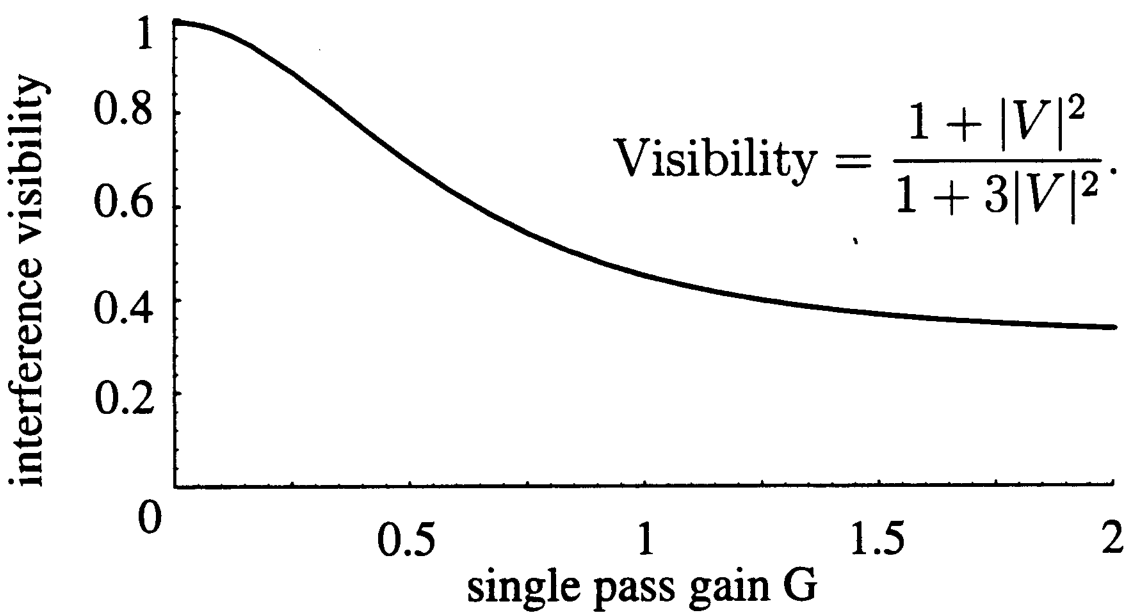

Ou, Zou, Wang, Mandel, Phys. Rev. A 42, 2957, 2000.

Conclusion: Some but not all of the quantum statistical features of the spontaneous parametric down conversion are preserved in the output of an unseeded, high-gain optical parametric amplifier.*

But why?

*Nagasako, Bentley, Boyd, and Agarwal, accepted for publication in PRA

Processes Contributing to the Coincidence Count Rate

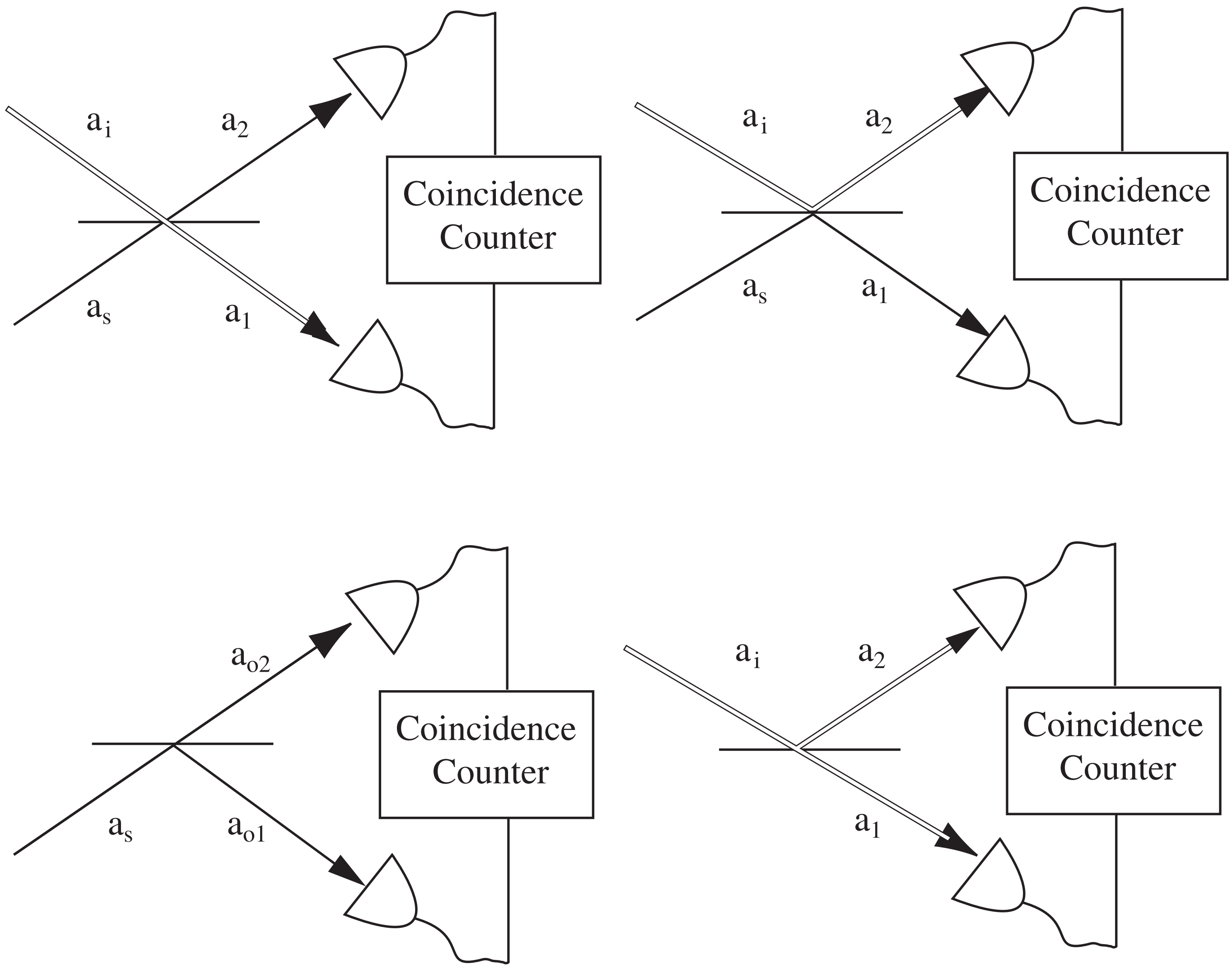

(And interference among these processes!)

General Treatment of Nonclassical Interferometers

Input/Output Relation of Interferometer

$$\begin{pmatrix} \hat{a}_1 \\ \hat{a}_2 \end{pmatrix} = \begin{pmatrix} A & B \\ C & D \end{pmatrix} \begin{pmatrix} \hat{a}_s \\ \hat{a}_i \end{pmatrix}$$

Direct Output $\quad A = D = 1 \quad B = C = 0.$

Beam Splitter $\quad A = D = \dfrac{1}{\sqrt{2}} \qquad B = C = \dfrac{-i}{\sqrt{2}}$

Quantum Litho. $\quad A = C = \dfrac{1}{\sqrt{2}} - \dfrac{i}{\sqrt{2}} e^{i\chi} \quad B = D = -\dfrac{i}{\sqrt{2}} + \dfrac{1}{\sqrt{2}} e^{i\chi}$

Coincidence Detection Rate

$$\begin{aligned}
\langle \hat{a}_1^\dagger \hat{a}_2^\dagger \hat{a}_2 \hat{a}_1 \rangle = \quad & |C|^2 |A|^2 \langle \hat{a}_s^\dagger \hat{a}_s^\dagger \hat{a}_s \hat{a}_s \rangle \\
& + |D|^2 |A|^2 \langle \hat{a}_s^\dagger \hat{a}_i^\dagger \hat{a}_i \hat{a}_s \rangle \\
& + |C|^2 |B|^2 \langle \hat{a}_i^\dagger \hat{a}_s^\dagger \hat{a}_s \hat{a}_i \rangle \\
& + |D|^2 |B|^2 \langle \hat{a}_i^\dagger \hat{a}_i^\dagger \hat{a}_i \hat{a}_i \rangle \\
& + 2 \text{ Re } A^* C^* D A \langle \hat{a}_s^\dagger \hat{a}_s^\dagger \hat{a}_i \hat{a}_s \rangle \\
& + 2 \text{ Re } A^* C^* C B \langle \hat{a}_s^\dagger \hat{a}_s^\dagger \hat{a}_s \hat{a}_i \rangle \\
& + 2 \text{ Re } A^* C^* D B \langle \hat{a}_s^\dagger \hat{a}_s^\dagger \hat{a}_i \hat{a}_i \rangle \\
& + 2 \text{ Re } A^* D^* C B \langle \hat{a}_s^\dagger \hat{a}_i^\dagger \hat{a}_s \hat{a}_i \rangle \\
& + 2 \text{ Re } A^* D^* D B \langle \hat{a}_s^\dagger \hat{a}_i^\dagger \hat{a}_i \hat{a}_i \rangle \\
& + 2 \text{ Re } B^* C^* D B \langle \hat{a}_i^\dagger \hat{a}_s^\dagger \hat{a}_i \hat{a}_i \rangle
\end{aligned}$$

Interferometer-Dependent Coefficients of the Individual Contributions to the Joint Detection Probability

		OP	A	HOMI	QL
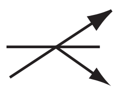	$\|C\|^2\|A\|^2$	0		1/4	(1+sin)^2
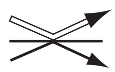	$\|D\|^2\|A\|^2$	1		1/4	1-sin ^{2}
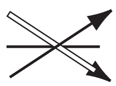	$\|C\|^2\|B\|^2$	0		1/4	1-sin ^{2}
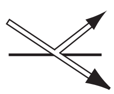	$\|D\|^2\|B\|^2$	0		1/4	(1-sin)^2
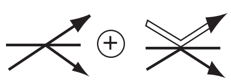	$2\ \mathrm{Re}\ A^*C^*DA$	0		0	2 cos (1+sin)
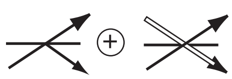	$2\ \mathrm{Re}\ A^*C^*CB$	0		0	2 cos (1+sin)
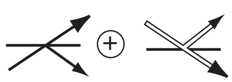	$2\ \mathrm{Re}\ A^*C^*DB$	0		1/2	2 cos ^{2}
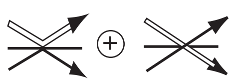	$2\ \mathrm{Re}\ A^*D^*CB$	0		-1/2	2 (1-sin ^{2})
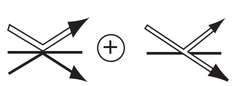	$2\ \mathrm{Re}\ A^*D^*DB$	0		0	2 cos (1-sin)
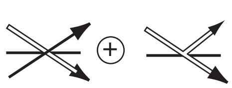	$2\ \mathrm{Re}\ B^*C^*DB$	0		0	2 cos (1-sin)

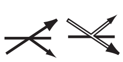 single-input terms = both detected photons arise from a single input arm

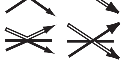 dual-input terms = detected photons arise from both input arms

Quantum Expectation Values of the Individual Contributions to the Joint Detection Probability

		$\lvert 1\,1\rangle$	$\lvert m\,m\rangle$	$\lvert \alpha_0\,\alpha_0\rangle$	OPA
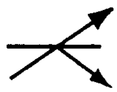	$\langle a_s^\dagger a_s^\dagger a_s a_s\rangle$	0	m(m-1)	$\lvert\alpha_0\rvert^4$	$2(\bar{m})^2$
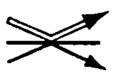	$\langle a_s^\dagger a_i^\dagger a_i a_s\rangle$	1	m^2	$\lvert\alpha_0\rvert^4$	$2(\bar{m})^2 + \bar{m}$
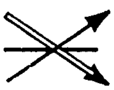	$\langle a_i^\dagger a_s^\dagger a_s a_i\rangle$	1	m^2	$\lvert\alpha_0\rvert^4$	$2(\bar{m})^2 + \bar{m}$
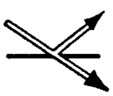	$\langle a_i^\dagger a_i^\dagger a_i a_i\rangle$	0	m(m-1)	$\lvert\alpha_0\rvert^4$	$2(\bar{m})^2$
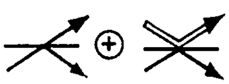	$\langle a_s^\dagger a_s^\dagger a_i a_s\rangle$	0	0	$\lvert\alpha_0\rvert^4$	0
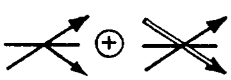	$\langle a_s^\dagger a_s^\dagger a_s a_i\rangle$	0	0	$\lvert\alpha_0\rvert^4$	0
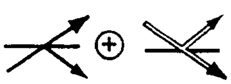	$\langle a_s^\dagger a_s^\dagger a_i a_i\rangle$	0	0	$\lvert\alpha_0\rvert^4$	0
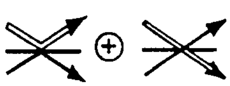	$\langle a_s^\dagger a_i^\dagger a_s a_i\rangle$	1	m^2	$\lvert\alpha_0\rvert^4$	$2(\bar{m})^2 + \bar{m}$
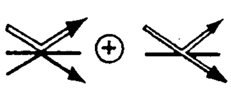	$\langle a_s^\dagger a_i^\dagger a_i a_i\rangle$	0	0	$\lvert\alpha_0\rvert^4$	0
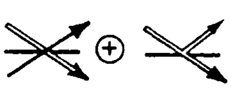	$\langle a_i^\dagger a_s^\dagger a_i a_i\rangle$	0	0	$\lvert\alpha_0\rvert^4$	0

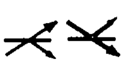 single-input terms = both detected photons arise from a single input arm

 dual-input terms = detected photons arise from both input arms

Nature of Decreased Fringe Visibility in a High-Gain Optical Parametric Amplifier

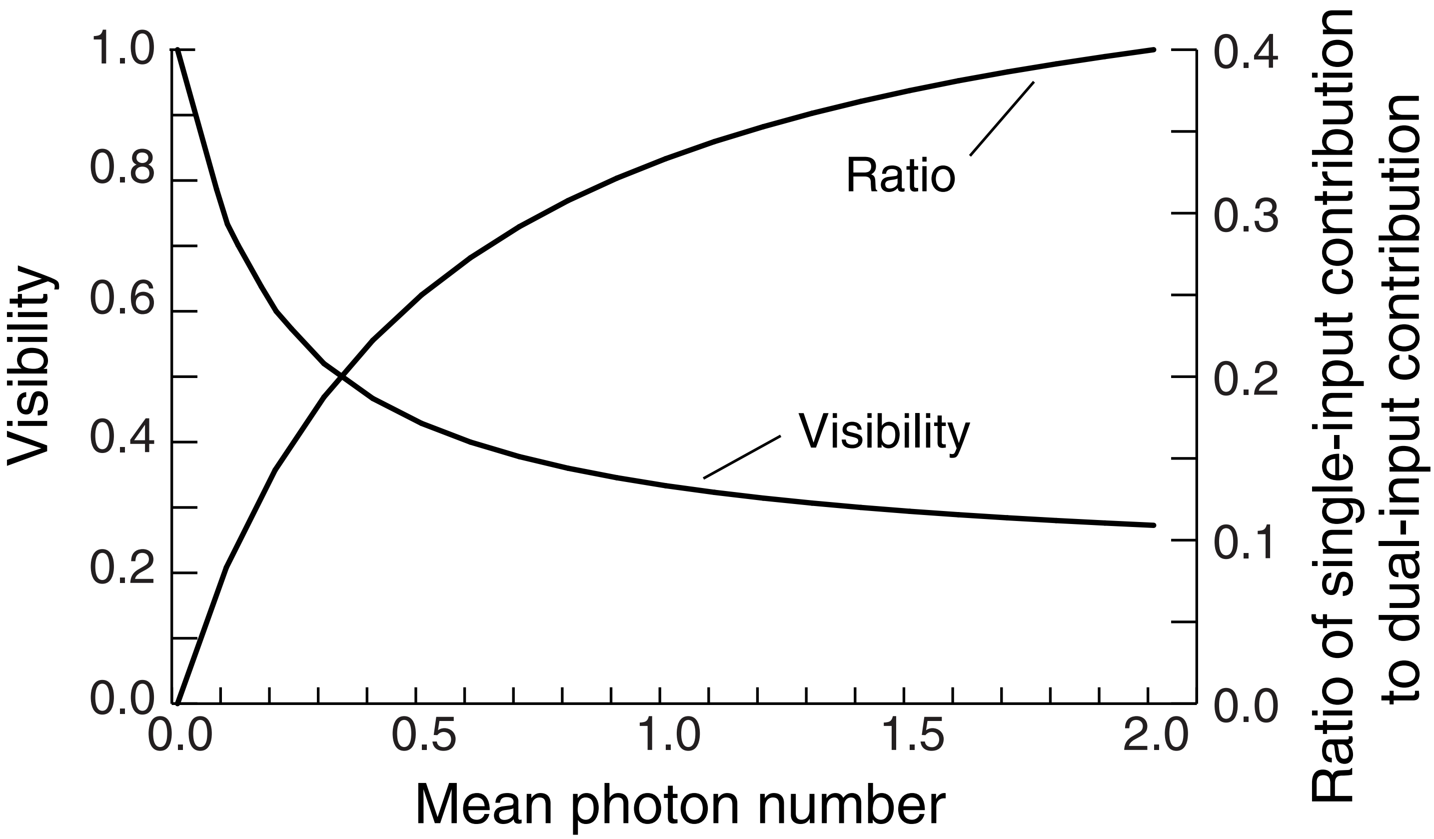

TWO ROUTES TO ENTANGLEMENT

$\chi^{(2)}$

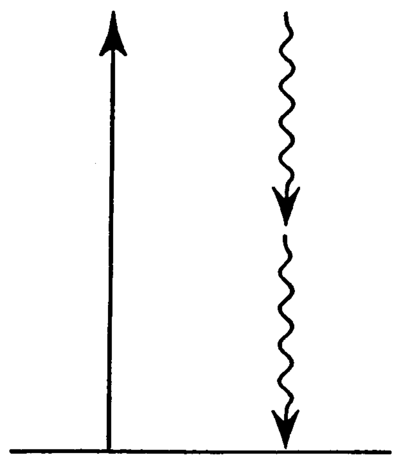

$\chi^{(3)}$

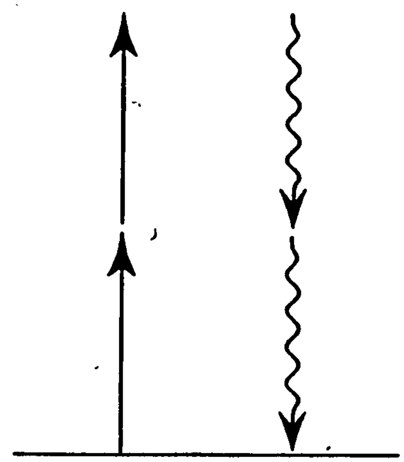

Generation of Squeezed Light by use of EIT

Robert W. Boyd and C. R. Stroud, Jr., University of Rochester

Three Approaches

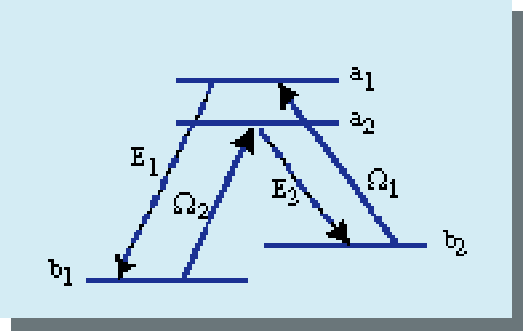

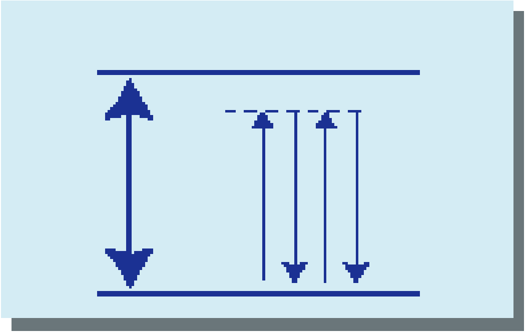

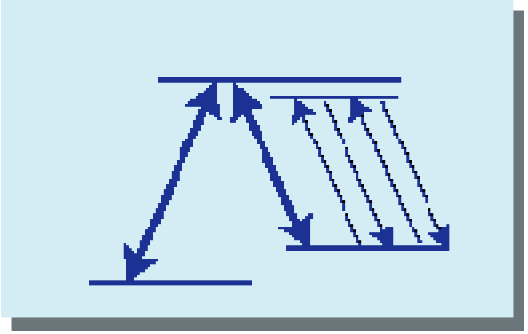

Fundamental idea: EIT eliminates linear absorption so that there is no spontaneous emission background noise.

Application of Two-Level EIT to Squeezed-Light Generation

- Squeezing by self-phase modulation

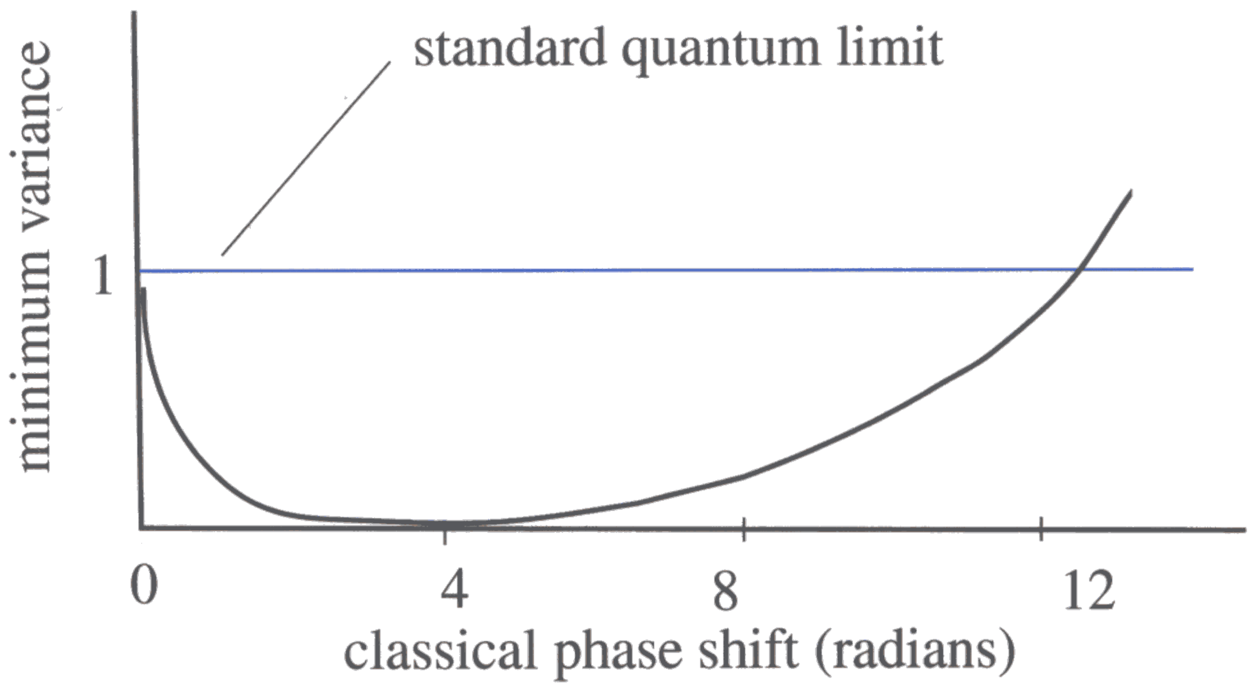

Blow, Loudon, and Phoenix, J. Mod. Opt., 40, 2515, 1993

EIT allows phase shifts large enough to produce significant squeezing, and prevents signal-beam absorption which can degrade the squeezing.

Honey Comb Pattern Formation

Robert W. Boyd and C. R. Stroud, Jr., University of Rochester

Output from cell with single gaussian beam input

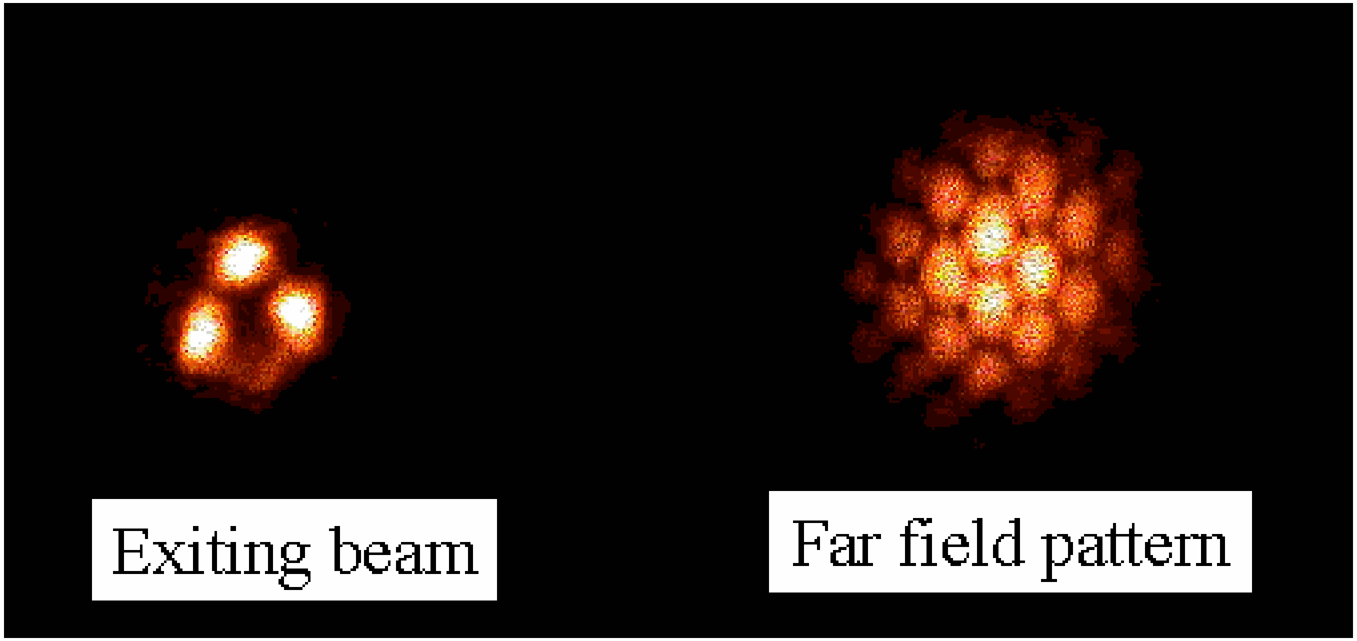

Quantum image?

Input power 150 mW
Input beam diameter 0.22 mm
$\lambda = 588.995$ nm

Sodium vapor cell
$T = 220°$ C

Some Related Findings

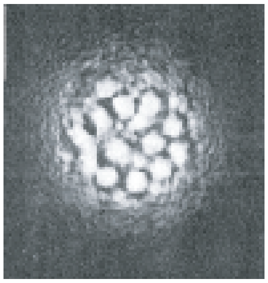

- spontaneous pattern formation in nematic LC with mirror feedback

R. MacDonald and H.J. Eichler, Opt. Comm. **89** (1992) 289-295.

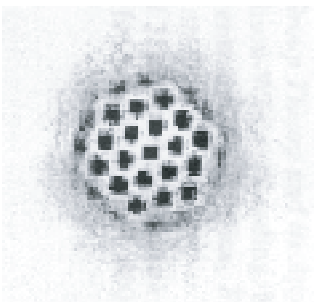

- simulation of pattern formation in a Kerr slice with mirror feedback

F. Papoff, G. D'Alessandro, G.-L. Oppo, and W.J. Firth, Phys. Rev. A **48** (1993) 634.

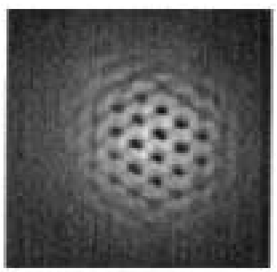

- spontaneous pattern formation in sodium vapor with a feedback mirror

R. Herrero, E. Grosse Westhoff, A. Aumann, T. Ackemann, Y. A. Logvin, and W. Lange, Phys. Rev. Lett. **82** (1999) 4627.

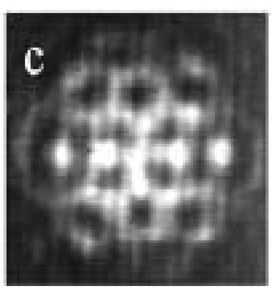

- spontaneous pattern formation in a near-degenerate OPO

M. Vaupel, A. Maitre, and C. Fabre, Phys. Rev. Lett. **83** (1999) 5278.

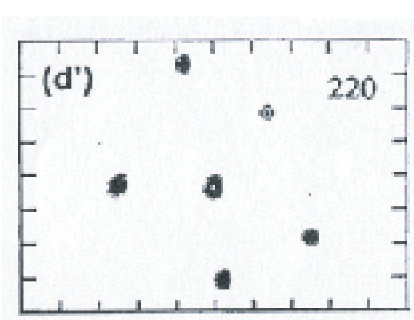

- filementation of an aberrated beam in sodium vapor

J.W. Grantham, H.M. Gibbs, G. Khitrova, J.F. Valley, and Xu Jiajin, Phys Rev. Lett. **66** (1991) 1422.

Experimental Results

Frequency dependence

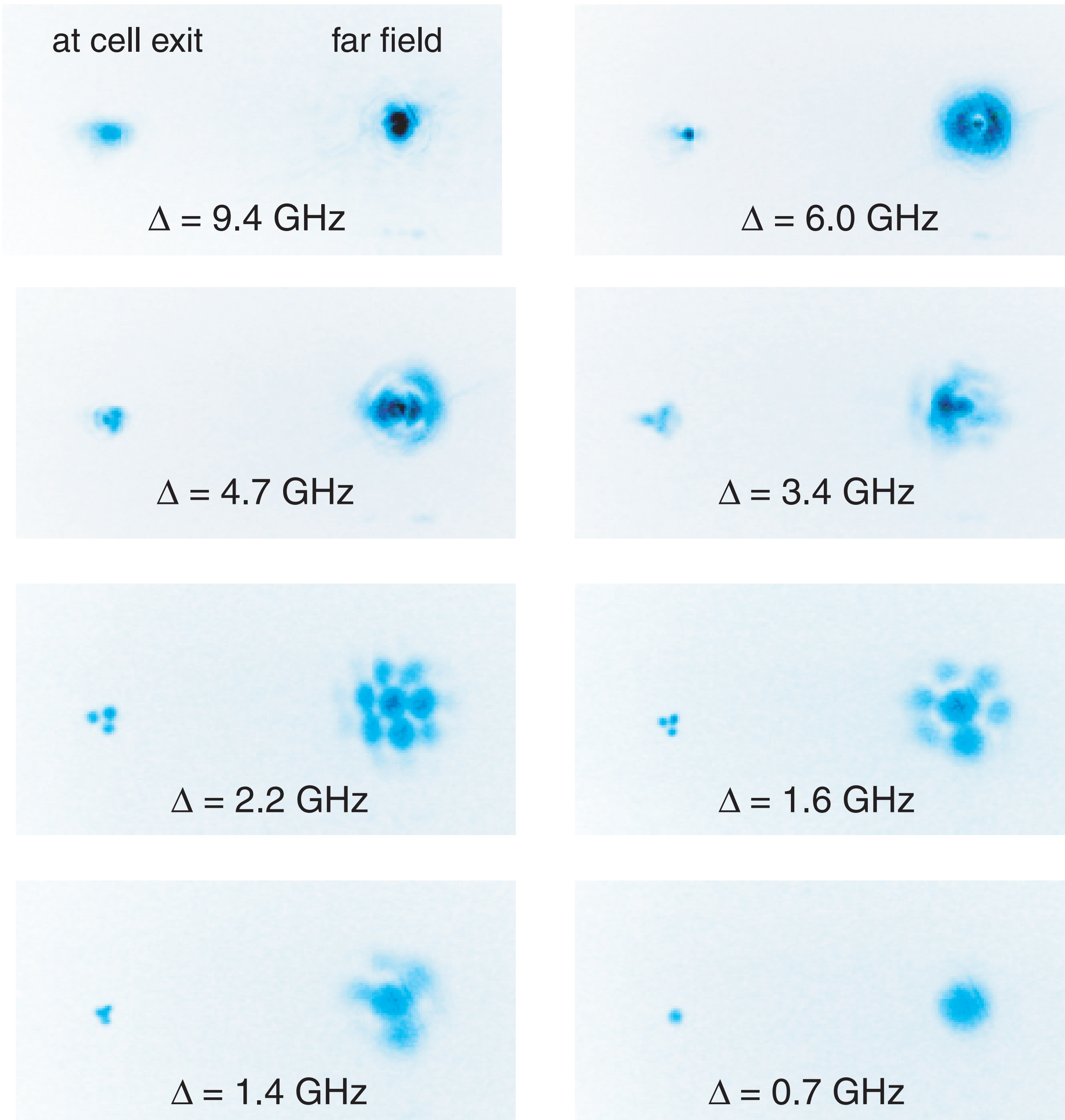

$N = 3 \times 10^{12}\ \mathrm{cm}^{-3}$, $P = 110$ mW, $2w = 180\ \mu$m

Spontaneous Pattern Formation in Sodium Vapor

A sodium vapor may be thought of as a medium composed of two-level atoms. Light whose frequency is near the atomic transition frequency experiences a refractive index n which depends strongly on the intensity I:

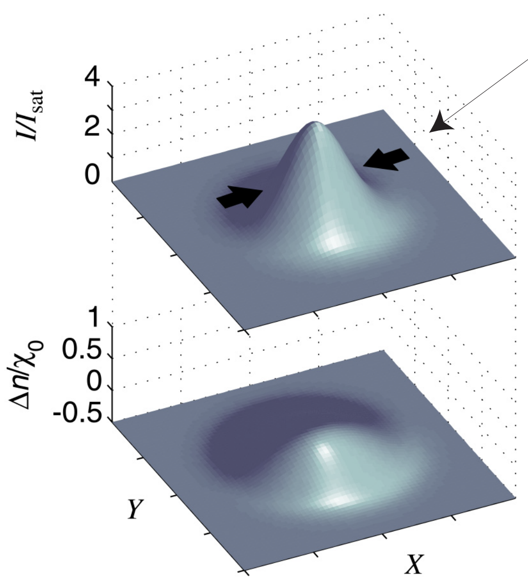

$$n = 1 + \quad n$$

$$1 + \frac{1}{2}\,\frac{0}{1 + I/I_{sat}}$$

Since light refracts in the direction of increasing index, in a medium with negative saturable nonlinearity it refracts toward regions of higher intensity. This causes smooth beams to narrow or self-focus. But it also tends to destabilize a beam as small amplitude fluctuations grow due to local self-focusing. Thus beams with even small amplitude noise can spontaneously split into two or more separate beams.

*For sodium at 200°C, $_0$ -0.05 and I_{sat} 6 mW/cm²

A simulation of spontaneous break-up into 3 stable beams:

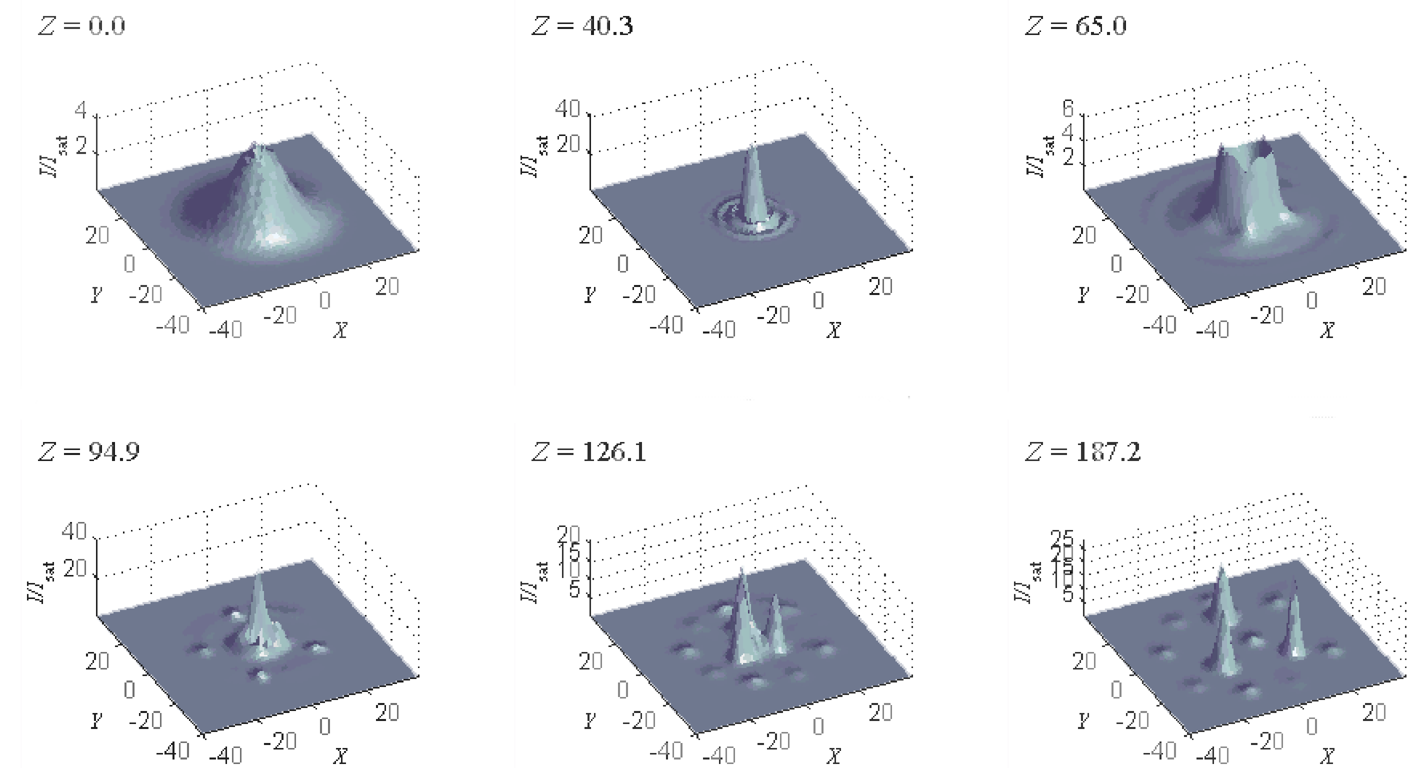

Experimental observation of spontaneous break-up resulting in a striking far-field pattern:

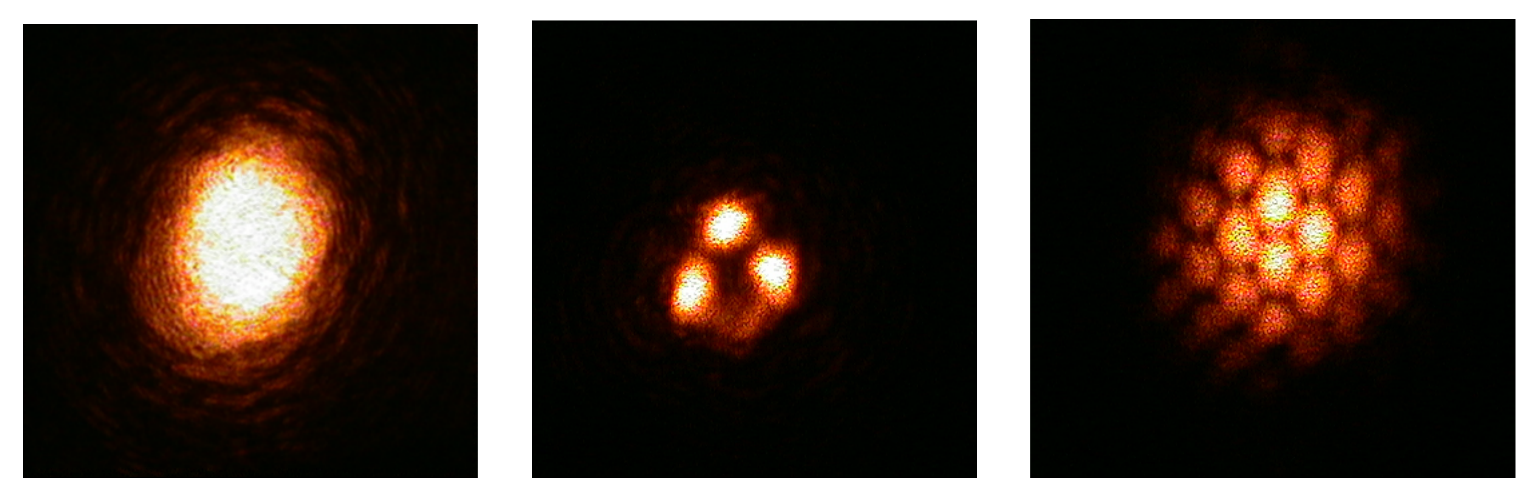

beam entering sodium

beam leaving sodium

far-field pattern

Pictures taken by R. Bennink, S. Lukishova, and V. Wong.

Some Underlying Issues in Nonlinear Optics

- Self-Assembly/Self-Organization in Nonlinear Systems
- Stability vs. Instability (and Chaos) in Nonlinear Systems

Chaos in Sodium Vapor

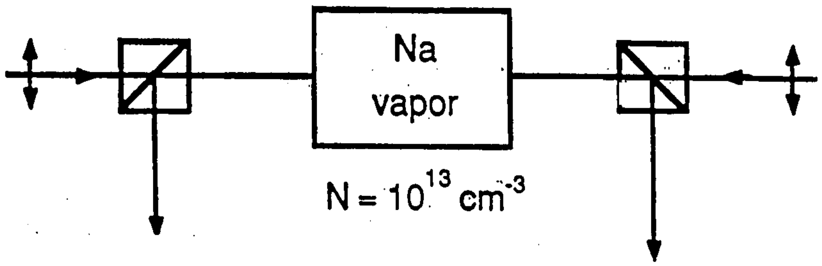

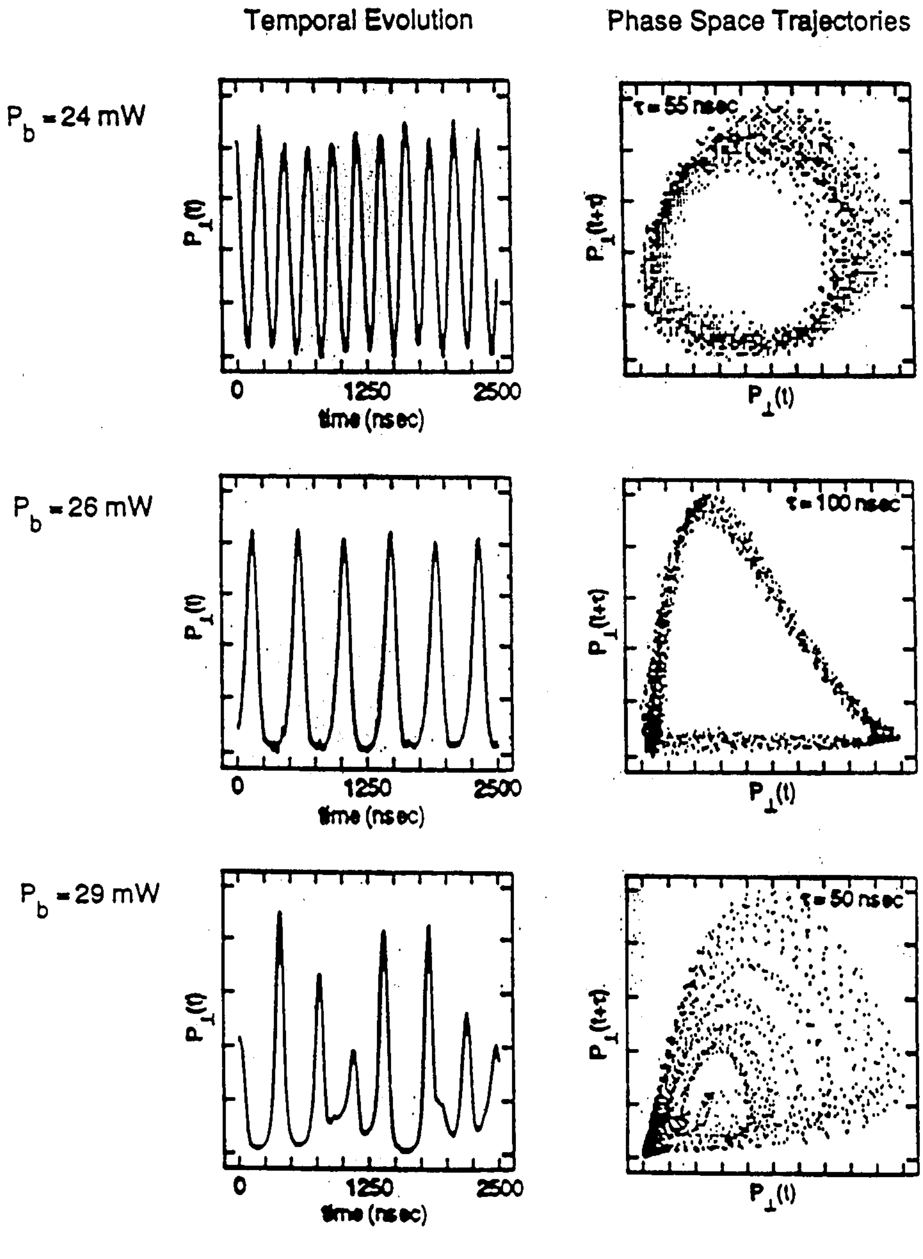

PRL 58, 2432 (1987); 61, 1827 (1988); 64 1721 (1990).

Laser Beam Filamentation

Spatial growth of wavefront perturbations

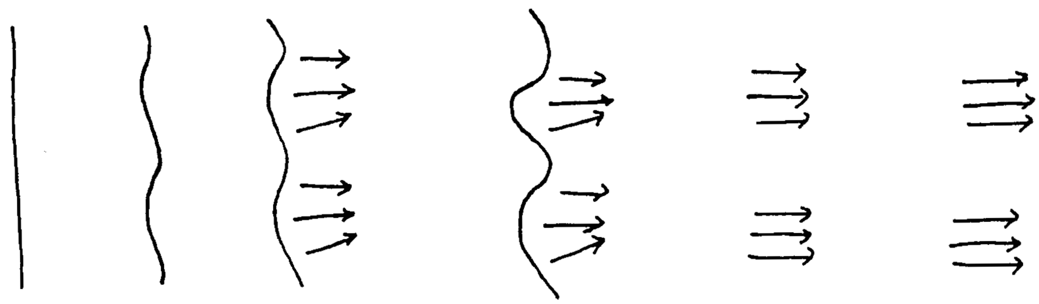

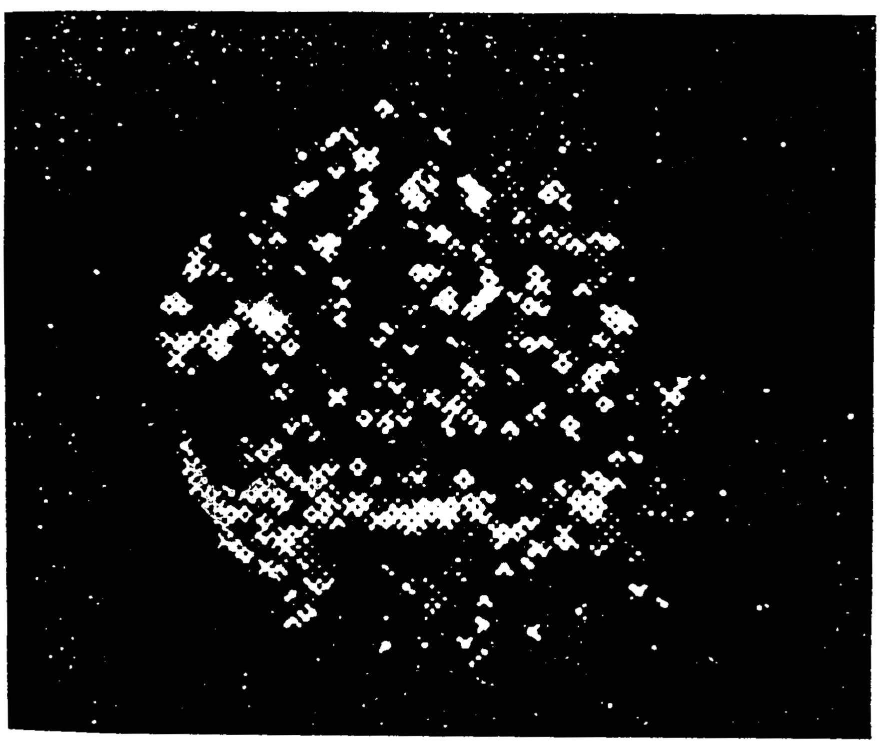

Fig. 17.2 Image of small-scale filaments at the exit windows of a CS_2 cell created by self-focusing of a multimode laser beam. [After S. C. Abbi and H. Mahr, *Phys. Rev. Lett.* 26, 604 (1971).]

Honey Comb Pattern Formation

Robert W. Boyd and C. R. Stroud, Jr., University of Rochester

Output from cell with single gaussian beam input

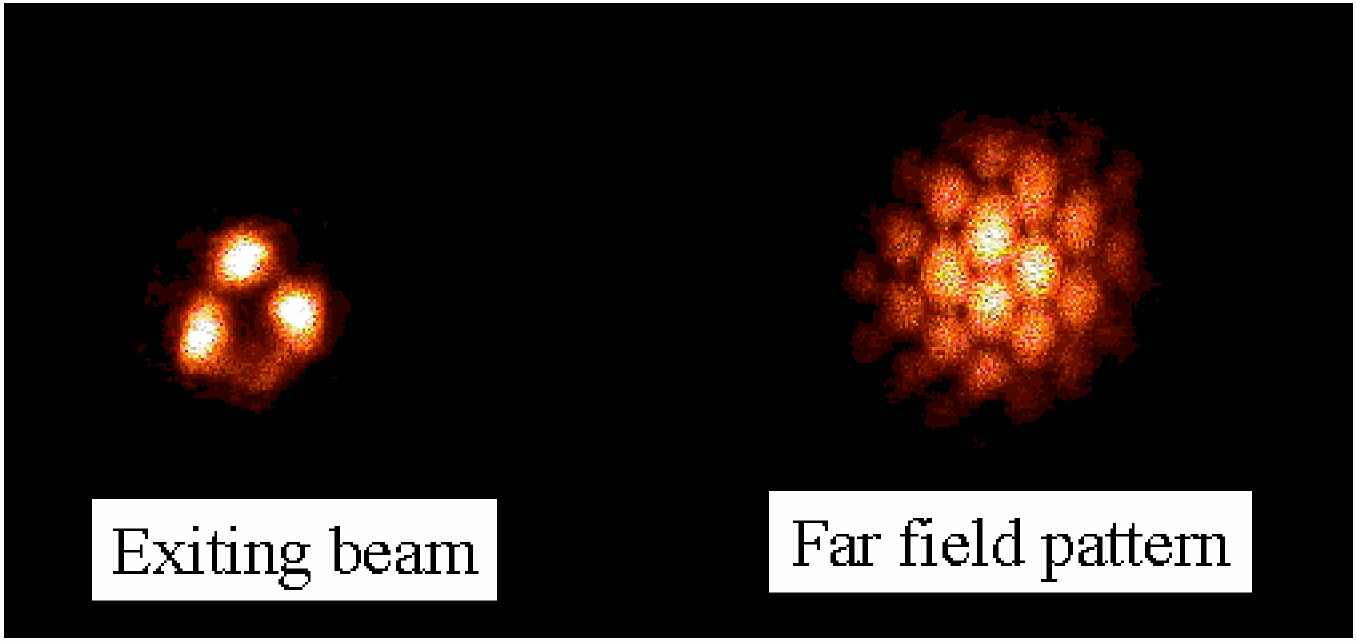

Quantum image?

Input power 150 mW
Input beam diameter 0.22 mm
$\lambda = 588.995$ nm

Sodium vapor cell
$T = 220^{\circ}$ C

Experiment in Self Assembly

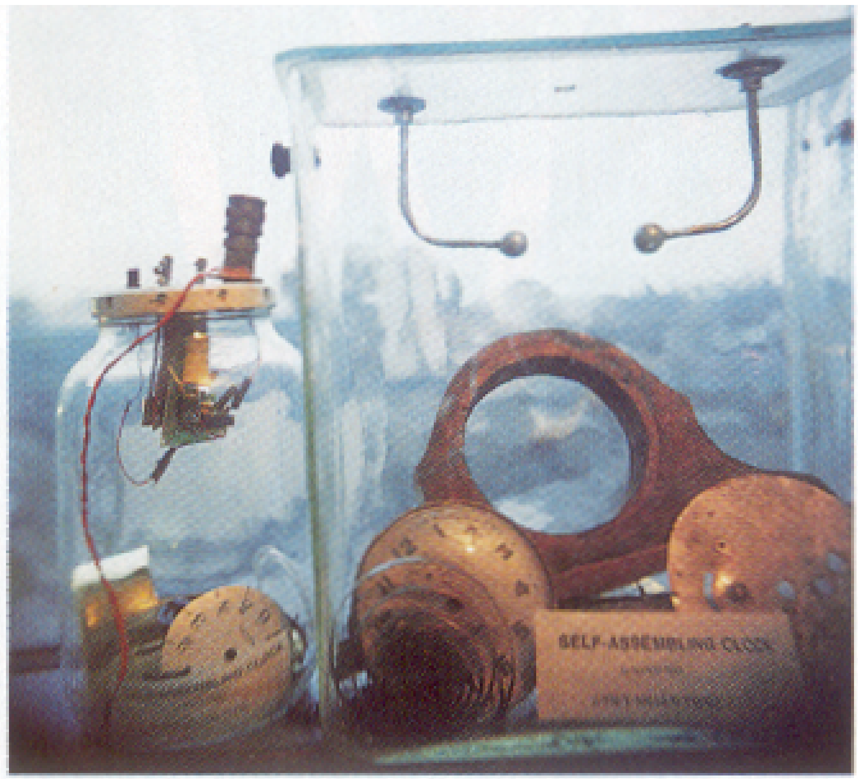

Joe Davis, MIT

Nanofabrication

- Materials (artificial materials)
- Devices

(distinction?)

Ultrafast All-Optical Switch Based On Arsenic Triselenide Chalcogenide Glass

- We excite a whispering gallery mode of a chalcogenide glass disk.

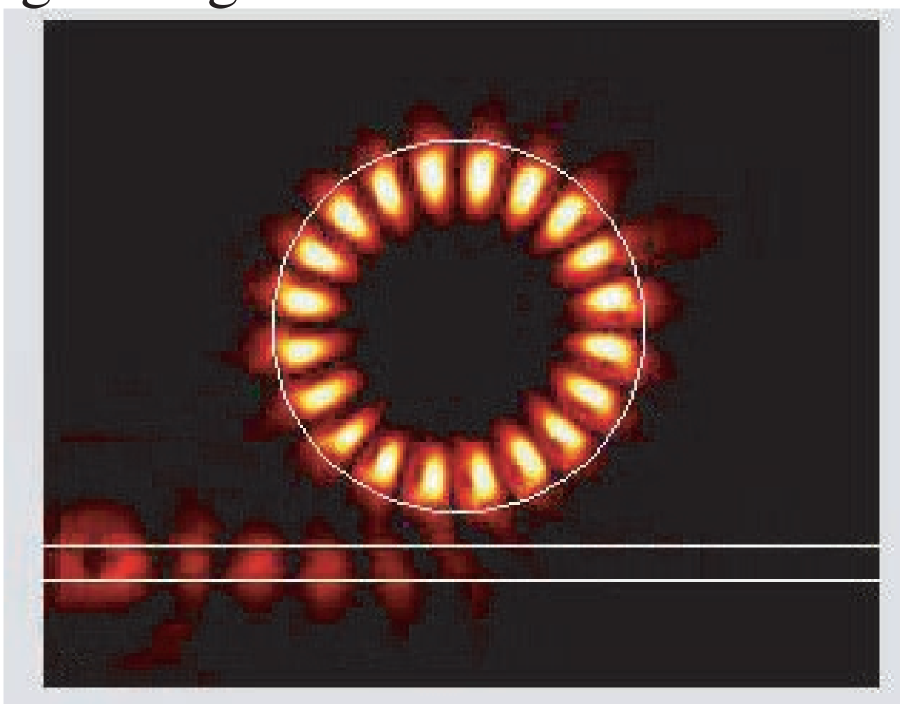

- The nonlinear phase shift scales as the square of the finesse F of the resonator. ($F \approx 10^2$ in our design)

- Goal is 1 pJ switching energy at 1 Tb/sec.

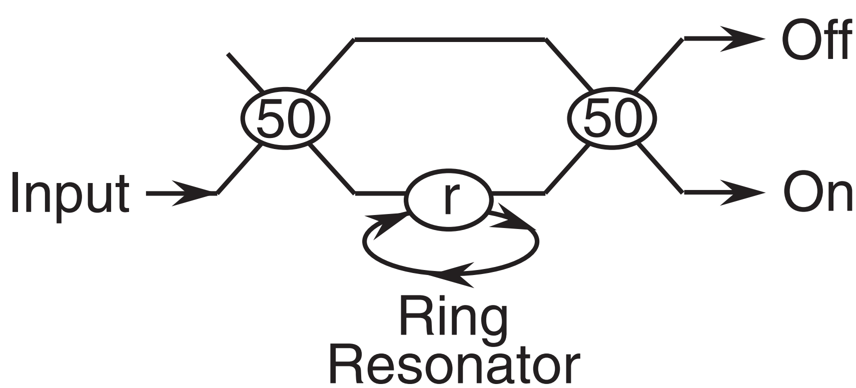

J. E. Heebner and R. W. Boyd, Opt. Lett. 24, 847, 1999.
(implementation with Dick Slusher, Lucent)

A Real Whispering Gallery

St. Paul's Cathedral, London

NLO of SCISSOR Devices

(Side-Coupled Integrated Spaced Sequence of Resonators)

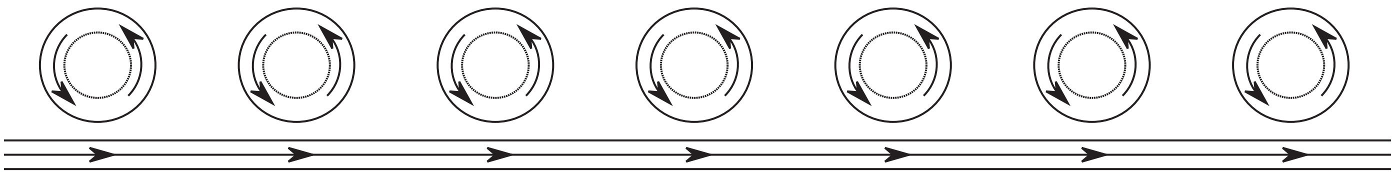

Displays slow-light, tailored dispersion, and optical solitons.
Description by NL Schrodinger eqn. in continuum limit.

- Pulses spread when only dispersion is present

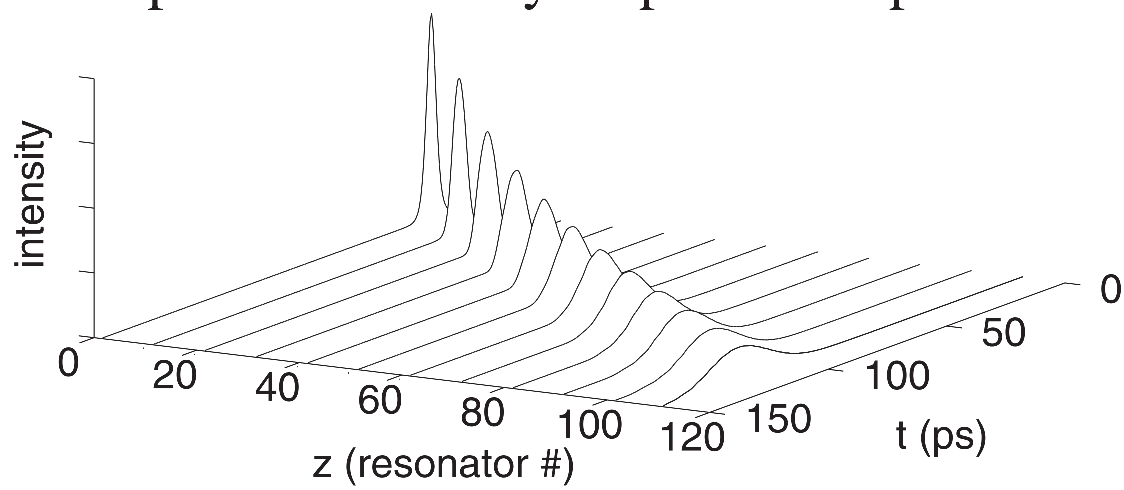

- But form solitons through balance of dispersion and nonlinearity

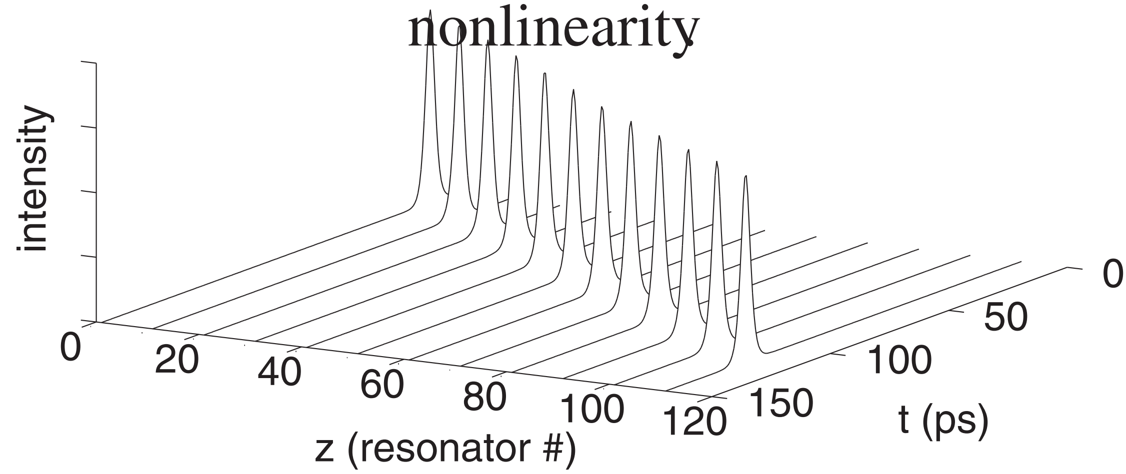

(J.E. Heebner, Q-Han Park and RWB)

Center for Biochemical Optoelectronic Microsystems

Cornell, Harvard, University of Rochester

Disk Resonator for the Detection of Biological Pathogens

R. Boyd, J. Heebner

Objective:

Obtain high sensitivity, high specificity detection of pathogens through optical resonance

Approach/Features:

Construct high-finesse whispering-gallery-mode disk resonator.

Presence of pathogen on surface leads to dramatic decrease in finesse.

Simulation of device operation: (FDTD)

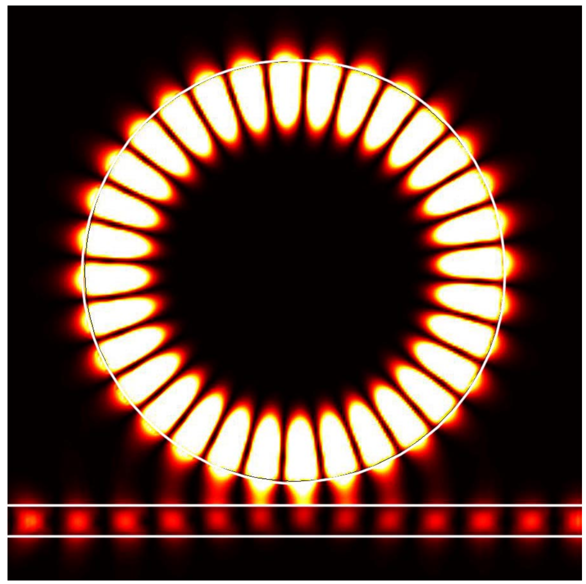

Intensity distribution in absense of absorber.

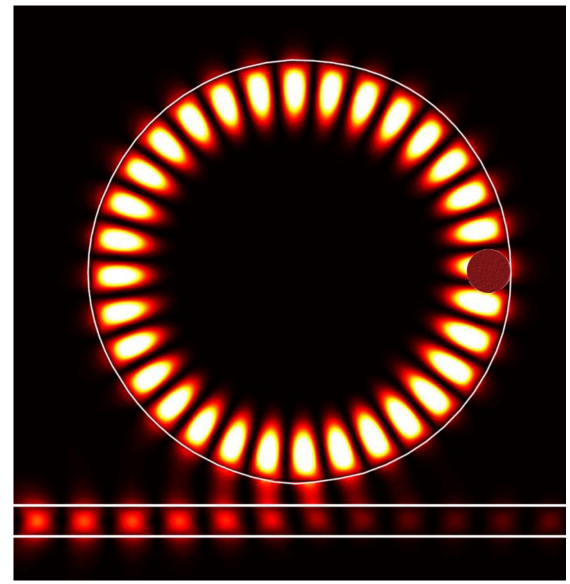

Intensity distribution in presence of absorber.

Progress:

Device design is complete.

Beginning fabrication

Nonlinear Optical Loop-De-Loop

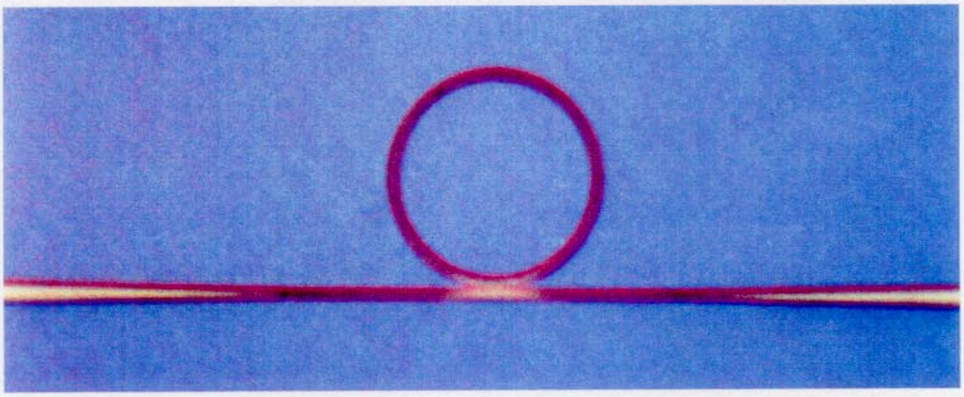

J.E. Heebner and R.W.B.